Available online at www.sciencedirect.com
ScienceDirect
Cement & Concrete Composites 28 (2006) 869–878
Cement & Concrete Composites
www.elsevier.com/locate/cemconcomp

Creep and durability of sand-coated glass FRP bars in concrete elements under freeze/thaw cycling and sustained loads

Kader Laoubi, Ehab El-Salakawy, Brahim Benmokrane *

Department of Civil Engineering, University of Sherbrooke, Sherbrooke, Qué., Canada J1K 2R1

Available online 12 September 2006

Abstract

This paper presents the test results of 21 concrete beams ($1800 \times 130 \times 180$ mm) reinforced with sand-coated glass FRP composite bars. The individual and coupled effects of freeze/thaw cycles and sustained bending stresses on the long-term behaviour of concrete beams reinforced with GFRP composite bars were investigated. The beams were exposed to 100, 200 and 360 freeze/thaw cycles (−20 °C to +20 °C) either in an unstressed state or loaded in bending to cause a tensile stress equals to 27% of the ultimate tensile strength of the GFRP bar. The conditioned beams were tested up to failure in a four-point bending set-up over a clear span of 1500 mm. The test results showed that the single or coupled action of freeze/thaw cycles and sustained bending stresses has no significant effect on the behaviour of the tested beams in terms of deflections, strains, and ultimate capacity. It was also concluded that the long-term deflections and the creep strain limits specified by ACI 440.1R-06 are conservative.

Keywords: Bond strength; Concrete beams; Creep; Freeze/thaw; Fiber reinforced polymer (FRP); Glass

1. Introduction

Fiber reinforced polymer (FRP) bars are used as reinforcement for concrete structures in which the corrosion of steel reinforcement has typically led to significant deterioration and rehabilitation needs. The use of FRP composites as reinforcement for such concrete structures provides a potential for increased service life, economic, and environmental benefits. The research on the durability of FRP composite materials is of great importance to establish their potential use in the field of construction. Among the different types, glass FRP composite bars has recently drawn much attention as reinforcement of concrete infrastructures due to its low cost compared to the other available types (carbon and aramid). The results of several studies [15,8,12,17,3,11,4] showed variety of factors, which can influence the durability of FRP materials as reinforcement for concrete structures. The research focusing on the durability of FRP materials is considered in an early stage especially due to the wide spectrum of durability issues and effects to be investigated [13,5,2]. The FRP can be damaged under certain physical (fatigue, creep, diffusion of humidity, extreme variation of the temperature) or chemical (alkaline environment) conditions. Freeze/thaw degradation is among the most important factors affecting cracked concrete members taking into account the fact that concrete is a permeable material. Thus, water could potentially accumulate at the FRP–concrete interface. As temperatures drop below freezing, the water will expand and as it crystallizes, it could potentially induce forces that will damage the bond between the FRP and concrete [18]. Furthermore, the large fluctuation of temperature through freeze/thaw cycles is expected to have an effect similar to that of the freezing water due to the difference in the coefficient of thermal expansion for the glass FRP bars in the transverse direction ($32–36 \times 10^{-6}$/°C) and concrete ($8–12 \times 10^{-6}$/°C). It should be noted that the coefficient of

* Corresponding author. Tel.: +1 819 821 7758; fax: +1 819 821 7974.
E-mail address: Brahim.Benmokrane@Usherbrooke.ca (B. Benmokrane).

0958-9465/$ - see front matter © 2006 Elsevier Ltd. All rights reserved.
doi:10.1016/j.cemconcomp.2006.07.014

Nomenclature

A_f	nominal cross-sectional area of FRP bars, mm^2
c_b	the distance from extreme compression fiber to neutral axis at balanced strain condition, mm
d	the distance from extreme compression fiber to centroid of main tension reinforcement, mm
d_b	nominal diameter of the reinforcing bar, mm
E_c	modulus of elasticity of concrete, GPa
E_f	modulus of elasticity of FRP bar, GPa
E_s	modulus of elasticity of steel, GPa
f'_c	compressive strength of concrete, MPa
f_{fu}	ultimate tensile strength of FRP reinforcing bars, MPa
f_y	yield strength of compression reinforcing steel, MPa
M_u	ultimate moment, kN m
β_1	depth reduction factor of the equivalent rectangular stress block
$\Delta_{(cp+sh)}$	the long-term deflection due to creep and shrinkage, mm
$(\Delta_i)_{sus}$	the immediate deflection due to creep and shrinkage under sustained loads, mm
ε_{cu}	the maximum usable compressive strain in the concrete (0.003)
ε_{fu}	the design rupture strain of the FRP reinforcement
ρ'	compressive steel reinforcement ratio
λ	Multiplier for additional long-term deflection
ξ	the time-dependant factor for sustained load (equals to 1.2 for 6 months of exposure to sustained loads)

thermal expansion for the glass FRP bars in the longitudinal direction is similar to that of concrete.

In addition, the long-term creep behaviour of FRP bars has not been specified by any design equation [9] and only long-term deflection equations for FRP-reinforced concrete members have been proposed. The presence of load has been identified as a major factor in the response of the FRP product to the harsh environments. Since pores in the resin may exist during fibers impregnation with resin, stress concentrations around these pores could occur under tensile loads, which results in micro-cracking of resin. Therefore an FRP bar, under tension, may sustain cracks in the matrix before rupture of fibers. Micro-cracks in the thin outer matrix skin cause a loss of tightness against the ingress of fluids giving greater access for the environment to attack the fibers. It was then concluded that any durability study has to be performed under sustain tensile stress to resemble field conditions.

Very limited experimental and analytical data is available on the effects of cold temperature or freeze/thaw action on concrete members reinforced with FRP bars [7]. Virtually no work has been done on the combined effects of freeze/thaw cycles and sustained load action on concrete members reinforced with FRP bars. The tests reported in this paper partially fill this void.

2. Research significance

Durability of FRP composites in general and especially glass FRP bars (with relatively low cost) is the most crucial element governing the life-cycle cost of FRP-reinforced concrete structures. Test results of a new extensive research program investigating the individual and simultaneous coupled effect of sustained loads and freeze/thaw cycling on the creep behaviour and durability of sand-coated glass FRP composite bars as reinforcement for concrete beams are presented.

3. Experimental program

The experimental program in this study focuses on investigating the individual and the coupled effect of freeze/thaw cycling and sustained loading on the creep and long-term behaviour of concrete beams reinforced with GFRP bars.

3.1. Glass FRP sand-coated bars

The GFRP bars used in this study are the second generation of GFRP [16] which are composed of 75.9 % E-glass fibers (by weight) in Vinyl ester resin (Fig. 1). The 9.5 mm-diameter bars were made of longitudinal glass fiber strands bounded together with a thermosetting vinyl ester resin using pultrusion process. The GFRP bars were subjected to a double surface treatment. The first treatment was carried out to increase the bond between the fibers and the resin, which would improve the durability properties

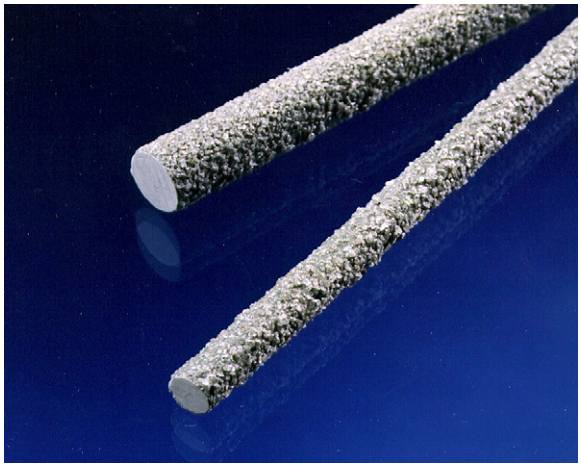

Fig. 1. Sand-coated glass FRP bars used in the current study.

Table 1
Tensile properties of the GFRP bars used in this study

Ultimate tensile strength	$f_{u,ave}$	647 ± 12 MPa
Guaranteed tensile strength	$f^*_{fu}(f^*_{fu} = f_{u,ave} - 3\sigma)$	611 MPa
Design tensile strength (ACI 440.1R-06)	$f_{fu} = C_E * f^*_{fu}, C_E = 0.7$	427 MPa
Modulus of elasticity	$E_{f,ave}$	36 ± 1 GPa
Ultimate strain	$\varepsilon_{u,ave}$	$1.80 \pm 0.1\%$
Guaranteed strain	$\varepsilon^*_u = \varepsilon_{u,ave} - 3\sigma$	1.50%
Design strain (ACI 440.1R-06)	$\varepsilon_u = C_E * \varepsilon^*_u$	1.05%
Allowable strain for creep (ACI 440.1R-06)	20% ε_u	0.21%
Coefficient of thermal expansion	Transverse	33.0×10^{-6}/°C
	Longitudinal	8.0×10^{-6}/°C

of the composite product. The second surface treatment was done by adding a layer of sand coating to the bars to improve the bond properties of the bars. Table 1 gives the main properties of the bars in terms of average ultimate tensile strength, modulus of elasticity and average ultimate tensile strain. The guaranteed and design tensile strengths and strains are also given based on ACI 440.1R-06, which gives an allowable creep strain limit of 2100 micro-strain under sustained loads. The mechanical properties of the used glass FRP bars were determined by performing the tensile tests on at least five GFRP bar samples.

3.2. Concrete properties

The beams were constructed using normal-weight concrete with a nominal maximum aggregate size of 20 mm and an average 28-day concrete compressive strength of 40 MPa. At least, six 100×200 mm concrete cylinders for each concrete batch were taken. Three cylinders were cured at room temperature and then tested in compression after 28 days, which gave an average of 40 MPa for all concrete batches. The other three cylinders were conditioned simultaneously with their corresponding beams under 100, 200 and 360 freeze/thaw cycles. After drying out for three days, the conditioned cylinders were tested in compression, which gave an average of 45–47 MPa. Table 2 lists the concrete mix constituents and properties.

Table 2
Properties of used concrete

Item	Quantity or ratio
Cement (Type 10)	380 kg/m^3
Natural sand	837 kg/m^3
Aggregate (2.5–10 mm)	290 kg/m^3
Aggregate (10–20 mm)	683 kg/m^3
Water	154 kg/m^3
Air entraining agent	60 ml/100 kg
Retarder	30 ml/100 kg
Workability agent	300 ml/100 kg
Water/cement ratio	0.4
Entrained air content	6.0 %
Slump	80 mm

3.3. Concrete beam specimens reinforced with glass FRP

A total of 21 concrete beams reinforced with glass FRP bars were constructed and cured in laboratory environment for at least 28 days before conditioning. The conditioning process included sustained loads for different periods (50, 100, and 180 days) at room temperature and sustained loads at different number of freeze/thaw cycles (100, 200, and 360 cycles). Since two freeze/thaw cycles per day were carried out it can be noted that the selected periods for applying the sustained loads 50, 100, and 180 days were corresponding to 100, 200, and 360 freeze/thaw cycles, respectively.

The beams were 1800 mm long, 130 mm wide, and 180 mm deep as shown in Fig. 2. A small clear concrete cover of 20 mm was selected to facilitate and accelerate the penetration of water (humidity) to the reinforcement level. Also, this small cover is sensitive to any tensile forces that could be developed during conditioning as a result of reducing the confinement of the GFRP bars. The test parameters were the number of freeze/thaw cycles, and sustained loads. In addition to the three unconditioned control beams of Series I, the conditioned specimens were divided into three series of six beams each based on the conditioning parameters; sustained loads only (Series II), freeze/thaw cycles only (Series III), and combined sustained loads and freeze/thaw cycles (Series VI). For each series, two identical beams (twin) were subjected to the same number of freeze/thaw cycles and/or sustained loading conditions. Table 3 lists the details of the test specimens. The designation of the specimens can be explained as follows. The letters BG refer to beams reinforced with glass FRP bars, S refers to sustained load, FT refers to freeze/thaw, numbers 1, 2 and 3 refer to age at testing 50, 100, and 180 days, respectively (corresponding to 100, 200 and 360 freeze/thaw cycles, respectively).

The test beams were designed to have an under-reinforced concrete section using two No. 10 GFRP bars ($d_b = 9.54$ mm; $A_f = 71.0$ mm^2) as bottom reinforcement (with an actual reinforcement ratio of 0.73%). For all beams, 10-mm diameter smooth steel bars ($d_b = 10$ mm – $A_s = 78.5$ mm^2) were used as top reinforcement and stirrups. This beam design was intended to have a flexure mode of failure by rupture of the GFRP bars. This mode of failure, utilizing the ultimate tensile capacity of the GFRP bars, would show any degradation of the tensile and bond properties of the composite material.

3.4. Instrumentation

For each beam, a total of 2 (5-mm long) and 5 (80-mm long) electrical resistance strain gauges were used to measure strains in GFRP reinforcing bars and in concrete, respectively. For GFRP bars, strains were measured at the mid-span of the two bottom bars, while for concrete the strains were measured in two locations: at mid-span

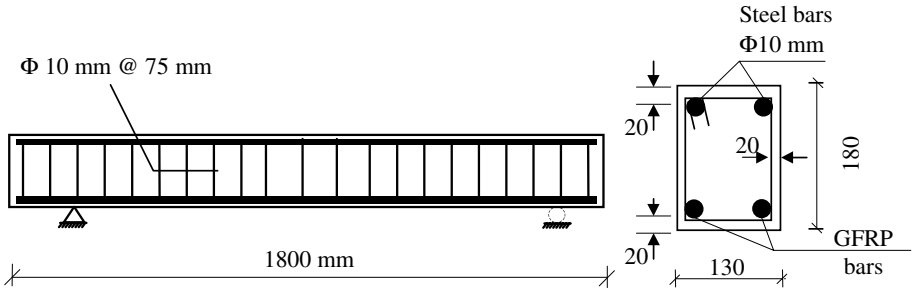

Fig. 2. Concrete dimension and reinforcing details for the tested beams.

Table 3
Details of the test specimens

Beams	Beam designation	Loading condition	Number of freeze/thaw cycles	Age at testing (days)
Series I (Reference)	BG-R1.1	No load	Room temperature	50
	BG-R2.1			100
	BG-R3.1			180
Series II	BG-S1.1	Sustained load	Room temperature	50
	BG-S1.2			
	BG-S2.1			100
	BG-S2.2			
	BG-S3.1			180
	BG-S3.2			
Series III	BG-FT1.1	No load	100	50
	BG-FT1.2			
	BG-FT2.1		200	100
	BG-FT2.2			
	BG-FT3.1		360	180
	BG-FT3.2			
Series VI	BG-SFT1.1	Sustained load	100	50
	BG-SFT1.2			
	BG-SFT2.1		200	100
	BG-SFT2.2			
	BG-SFT3.1		360	180
	BG-SFT3.2			

and at 200 mm from mid-span as shown in Fig. 3a. During conditioning of the specimens (under individual and coupled effect of sustained load and freeze/thaw cycles), dial gauges and hand-held 50× microscope were used to measure changes in mid-span deflections and crack widths, if there were any, respectively. During flexural tests, the dial gauges and the microscope were replaced with LVDTs at mid-span and at the location of the first two cracks (Fig. 3b).

3.5. Freeze/thaw cycling

Freeze/thaw cycling were performed at the environmental laboratory of the University of Sherbrooke's Civil Engineering Department (3.70×2.60 m environmentally-controlled chamber). The relative humidity was kept constant at 50% during all freeze/thaw cycles. During the freezing process, the lower bound was set to -20 °C for 6 h. During the thaw process, the temperature was raised to $+20$ °C for 6 h. This resulted in two freeze/thaw cycles per day. The freeze/thaw procedure was carried out in a similar manner to that of the US Army Cold Regions Research and Engineering Laboratory (CRREL) with heating and cool-down ramps as shown in Fig. 4. It should be noted that the number of freeze/thaw cycles in the field could differ substantially based on geographic location.

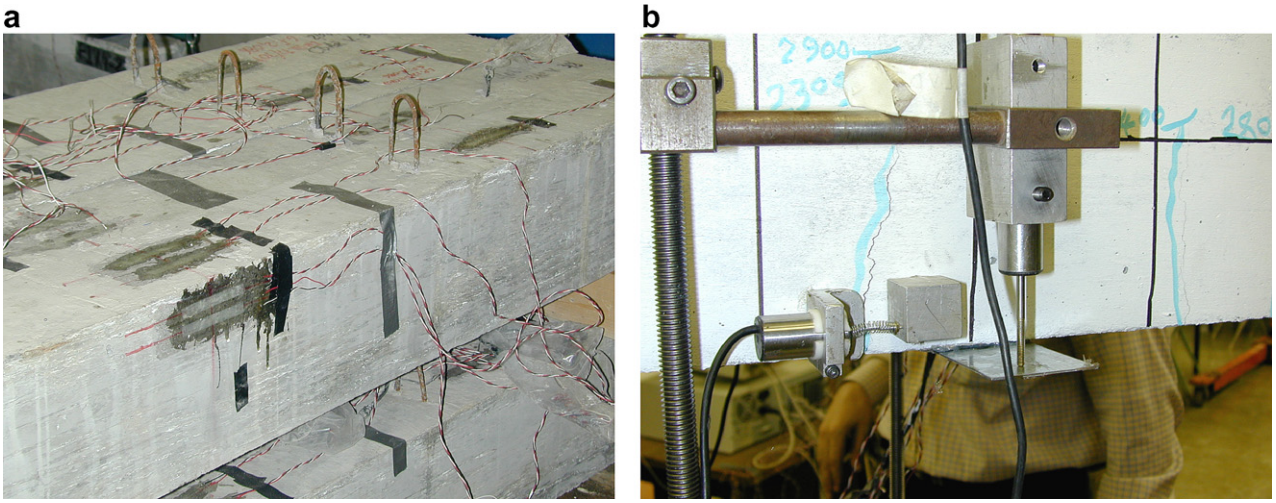

Fig. 3. External instrumentation: (a) concrete strain gauges, (b) LVDT's for deflection and crack width.

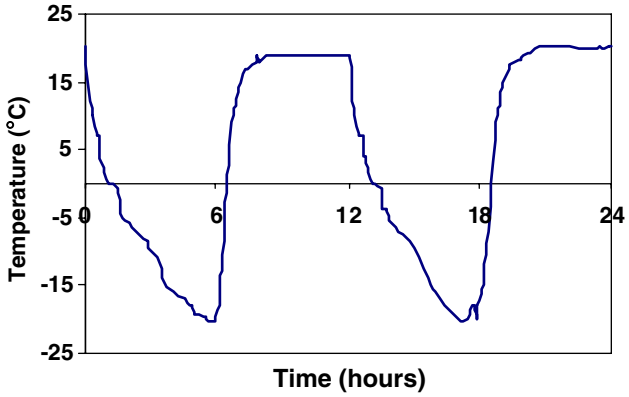

Fig. 4. Ramp rate for temperature change (freeze/thaw cycles).

Lesko [14] reported that on an average in Virginia there were 30 freeze/thaw cycles yearly. Soudki and Green [19] used a total of 50 freeze/thaw cycles in a study to simulate conditions in Canada whereas [10] reported reduction in flexure strength and modulus in their study on composites after 360 cycles which where used to simulate the life of the structure. The number of freeze/thaw cycles used in this study ranging from 100 to 360 cycles conservatively covers the life time of a structure in the cold regions of North America. No solution was used for the thaw period with the change in conditions being strictly controlled by temperature in the conditioning chamber alone.

3.6. Sustained loading

In this study, a new loading system for maintaining the concrete beam specimens under constant load (bending stresses) has been developed, designed, and fabricated at the University of Sherbrooke. The load was kept constant by a gravimetric force of a counterweight as shown in Fig. 5. A calibration for the applied load versus the counterweight was done for each loading system. One loading system (frame) can be used to apply constant load for up to four beam specimens. This loading system is suitable for all kinds of durability studied (moisture, freeze/thaw cycles, low and elevated temperatures, alkaline solutions, saline solutions) on reinforced concrete beams under sustained loads where space is limited. Because it is mobile (on wheels) and lightweight, it can be moved and installed easily into environmental chambers. This system has been successfully used by other researchers [6].

The sustained loads were applied to the concrete beams of phase I through four-point bending over a clear span of 1.50 m. A sustained moment, M_{sus}, of 3.70 kN m, which is equivalent to 1.4 times the theoretical cracking moment of the beam specimens ($M_{cr} = 2.66$ kN m). This sustained load caused an initial strain of approximately 4900 micro-strain, which is more than double the creep strain limit (2100 micro-strain as listed in Table 1) suggested by [2] under sustained loads. This was done to explore the potentials of the material and evaluate how conservative the current code is.

3.7. Flexure test set-up and procedure

After reaching the specified number of freeze/thaw cycles and the corresponding periods of exposure to sustained loads, the conditioning process was stopped and beam specimens were allowed ample time to dry out (without sustained loads at room temperature) before being tested in flexure to failure. Then, all beams of the same series were tested under four-point bending over a simply supported clear span of 1.50 m, which is identical to the sustained loading set-up. The load was applied at a load-controlled rate of 2.0 kN/min to achieve failure in 25–30 min. Figs. 6 and 7 show a schematic drawing and a photo for the test set-up, respectively.

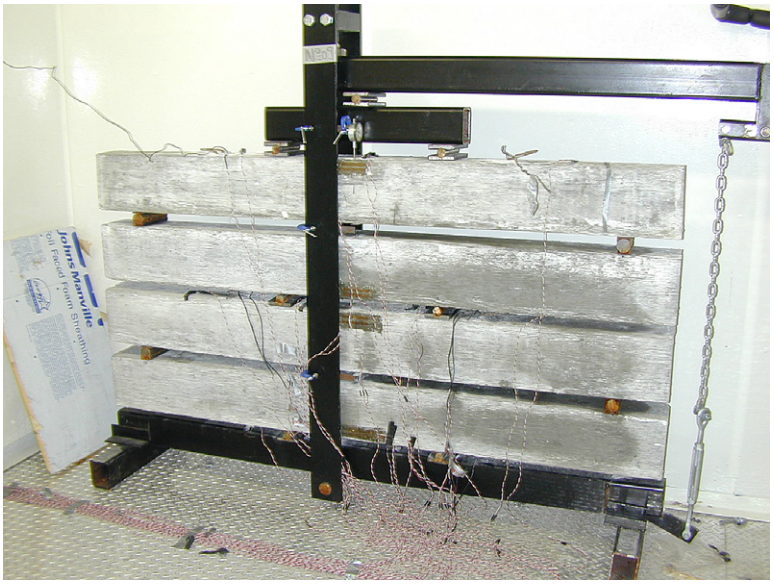

Fig. 5. Beams under sustained load and freeze/thaw cycles.

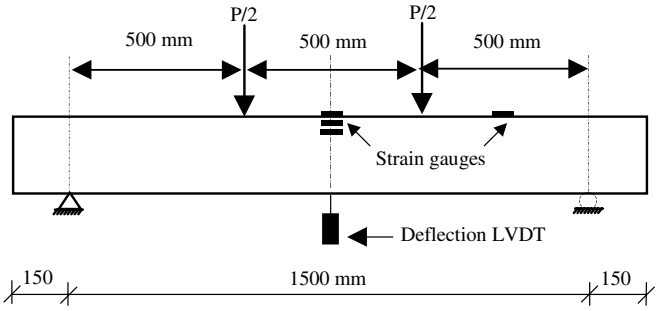

Fig. 6. Schematic drawing for the test set-up.

A simplified and conservative calculation of the nominal flexural capacity, M_n, of the test beams is given by the following equations [2]:

$$M_n = 0.8A_f f_{fu}\left(d - \frac{\beta_1 c_b}{2}\right) \quad (1)$$

$$c_b = \left(\frac{\varepsilon_{cu}}{\varepsilon_{cu} + \varepsilon_{fu}}\right) \quad (2)$$

The obtained nominal flexural capacity of the tested beams was 9.77 kN m, which is approximately 70% of the observed experimental value (average of 13.85 kN m for the unconditioned control beams).

4. Test results and discussion

The test results obtained from each twin beams were very similar, if not identical. Thus, only the results obtained from one of the twin beams are presented. The results will focus on deflection characteristics including immediate and long-term deflection, creep behaviour, and ultimate capacity. Also, the experimental results will be compared to the [2] expressions for long-term deflection and creep stain limits.

4.1. Behaviour of beams under sustained load

All beams subjected to sustained loads either at room temperature or at freeze/thaw cycling exhibited similar behaviour in terms of measured creep strain and long-term deflection. The mid-span deflection and the associated maximum measured strain increased with time. However, the rate of that increase was higher during the first 28 days than for the remaining period (22, 72, and 332 days). Fig. 8

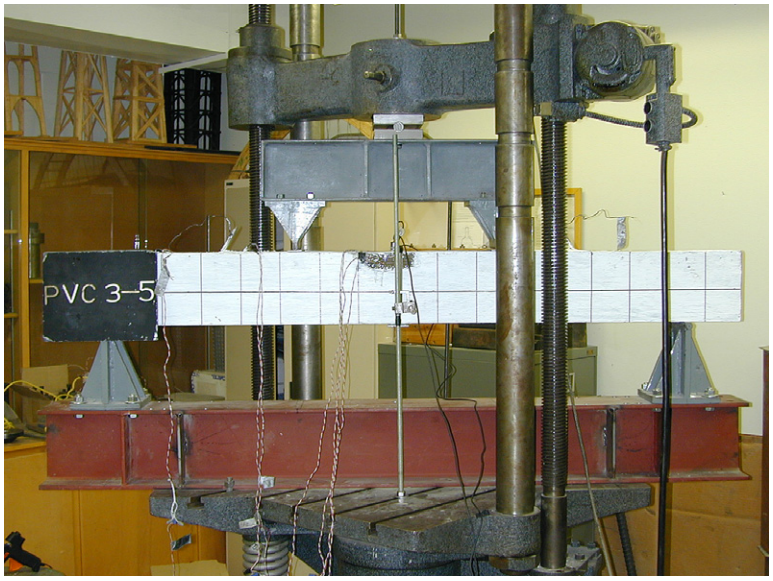

Fig. 7. Photo of the test set-up.

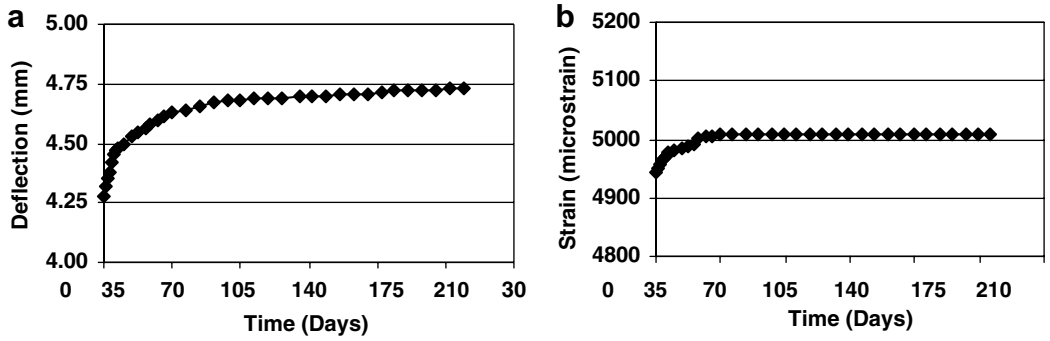

Fig. 8. Typical change in deflection and tensile strains in GFRP bars under sustained load (Specimen BG-S2): (a) change in deflection, (b) change in strain.

shows the typical mid-span deflection and strains in GFRP bars versus time, for beams under sustained loads for 180 days (beam BG-S2). It can be noted from Fig. 8a that, after 180 days of exposure to sustained loads, the overall mid-span deflection increased by 10.5%. Also, the associated maximum measured strain in the GFRP bars was increased by 1.9% (creep strain) as shown in Fig. 8b.

According to ACI 318-05 [1], Section 9.5.2.5, the long-term deflection due to creep and shrinkage, $\Delta_{(cp+sh)}$, can be computed according to these equations:

$$\Delta_{(cp+sh)} = \lambda(\Delta_i)_{sus} \quad (3)$$

$$\lambda = \frac{\xi}{1 + 50\rho'} \quad (4)$$

The ACI 440.1R-06 [2] introduced a modified expression for Eq. (3) taking into account for the differences in concrete compressive stress levels, lower elastic modulus and different bond characteristics of FRP bars. The value of λ was set equals to ξ as compression reinforcement is not considered for FRP-reinforced members ($\rho' = 0.0$).

$$\Delta_{(cp+sh)} = 0.6\xi(\Delta_i)_{sus} \quad (5)$$

Table 4 gives the predicted values of the long-term deflections due to creep and shrinkage according to Eq. (5) (using the experimental initial deflection) compared to the experimental values measured under sustained loading for 180 days (6 months). Since the tested beams have steel bars in the top compression zone, the values in Table 4 were calculated using the actual compression steel reinforcement ratio ($\rho' = 0.78\%$). This reduced the value of ξ (originally λ) from 1.2 to 0.86. It can be seen from Table 4 that Eq. (3) is highly over-estimating the measured deflections.

Table 4
Comparison of predicted and observed creep and shrinkage deflections of the beams under sustained loads for 26 weeks (6 months)

Beam	Instantaneous deflection (mm)	Deflection due to creep and shrinkage (mm)		
		δ_{Exp}	δ_{ACI}	$\delta_{ACI}/\delta_{Exp}$
BG-S3.1	4.28	0.45	2.18	4.84
BG-S3.2	4.32	0.44	2.23	5.07
BG-SFT3.1	4.41	0.44	2.28	5.18
BG-SFT3.2	4.38	0.45	2.27	5.04

4.2. Flexure test results (beams after conditioning)

In the following discussion, to define a reference for comparison purpose the service load of the beam is considered as approximately 40% of the average ultimate load of the control beams ($P_{ser} = 22.2$ kN and $M_{ser} = 5.6$ kN m). Table 5 gives a summary of the test results.

Fig. 9 shows load–deflection relationships for beams of series II conditioned under sustained loads compared to those of their control ones. The stressed beams, BG-S1, BG-S2 BG-S3, showed lower initial flexural stiffness than the corresponding control beams. This is due to the initial pre-cracking of these three beams under sustained load. However, with increasing the load above the level corresponding to the applied sustained load during conditioning, the stressed beams showed very similar flexural stiffness to those of their control. The average observed ultimate capacity decreased by 3.8%, 4.4% and increased by 6.8% due to conditioning under sustained loads for 50, 100, 180 days, respectively. However, at service load limit, the mid-span deflection increased by 2.2%, 1.4% and decreased by 1.1% for the beams conditioning under sustained loads for 50, 100, 180 days, respectively.

Fig. 10 shows the load–deflection relationships for beams of series III conditioned under freeze/thaw cycles compared to those of their control ones. Similar deflection behaviour was obtained for the four beams subjected to 100, 200 and 360 freeze/thaw cycles through the load history. At service load limit, the mid-span deflection increased by 3.6%, 0.1% and decreased by 2.5% for the beams conditioning under 100, 200, and 360 freeze/thaw cycles, respectively. However, the average measured

Table 5
Summary of test results

Beams		Ultimate moment		Max deflection at service		Max strain in FRP (%)	
		M_u (kN m)	Change (%)	δ (mm)	Change (%)	Service	Failure
Series I	BG-R1	13.9	N/A	8.06	N/A	4888	14,721
	BG-R2	13.8	N/A	9.33	N/A	4920	15,142
	BG-R3	13.8	N/A	7.78	N/A	4600	14,988
Series II	BG-S1	13.4	−4.05	8.24	2.3	4888	16,060
	BG-S2	13.2	−4.35	9.46	1.45	4877	15,493
	BG-S3	14.8	6.82	7.69	−1.14	4955	16,060
Series III	BG-FT1	14.7	5.35	7.86	−2.45	5702	15,185
	BG-FT2	13.7	−1.05	9.66	3.6	6617	17,412
	BG-FT3	14.2	2.90	7.79	0.10	5677	17,020
Series VI	BG-SFT1	13.7	−1.9	8.14	1.05	4719	14,466
	BG-SFT2	13.1	−5.45	9.27	−0.65	4991	16,935
	BG-SFT3	14.6	5.40	7.92	1.80	5005	15,214

ultimate capacity was increase by 2.8–5.3%. This can be attributed to an increase in concrete strength during conditioning (50% humidity) which was confirmed by testing concrete cylinders subjected to the same environmental conditions.

Fig. 11 shows the load–deflection relationships for beams of series VI conditioned under the coupled effect of sustained loads and freeze/thaw cycles compared to those of their control beams. The deflection behaviour for the beams of this series, BG-SFT1, BG-SFT2 and BG-SFT2 was very similar to those of series II under sustained loads only. The ultimate capacity of the stressed beams subjected to 100, 200, and 360 freeze/thaw cycles decreased by 1.9%, 5.4% and increased by 5.5%,

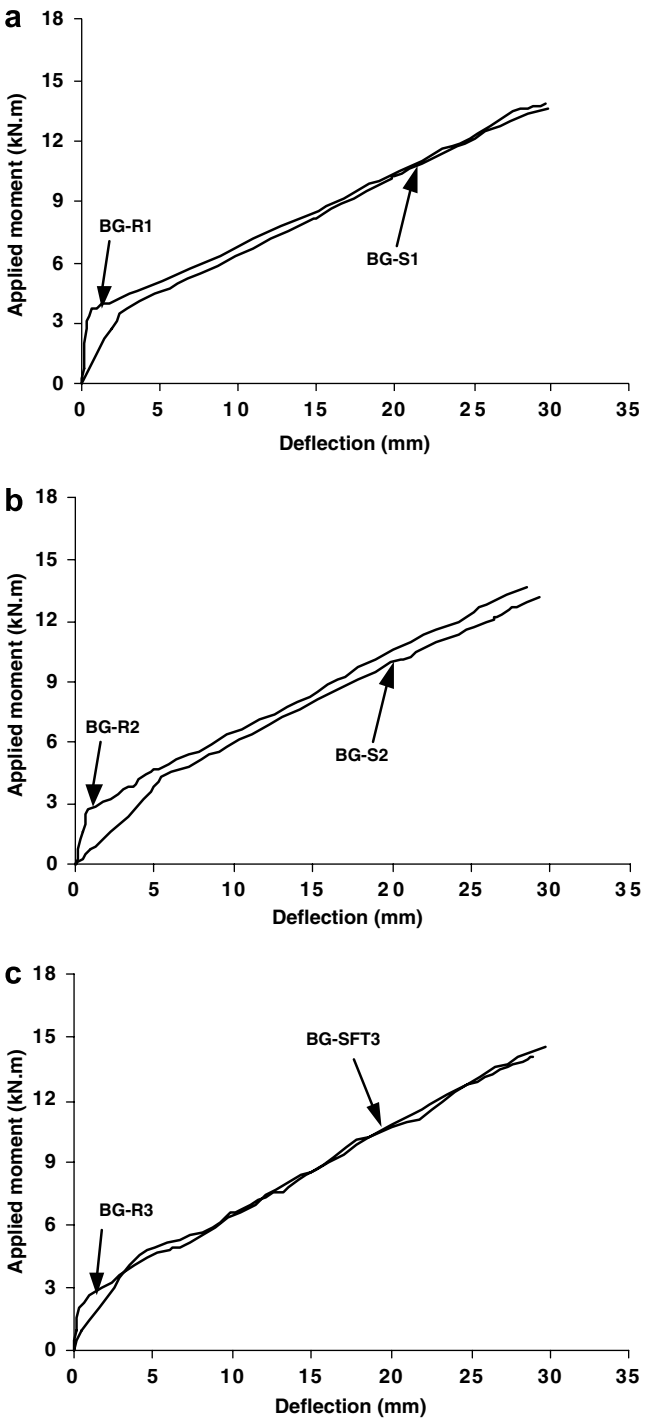

Fig. 9. Beams subjected to sustained loads (Series II): (a) 50 days, (b) 100 days, (c) 180 days.

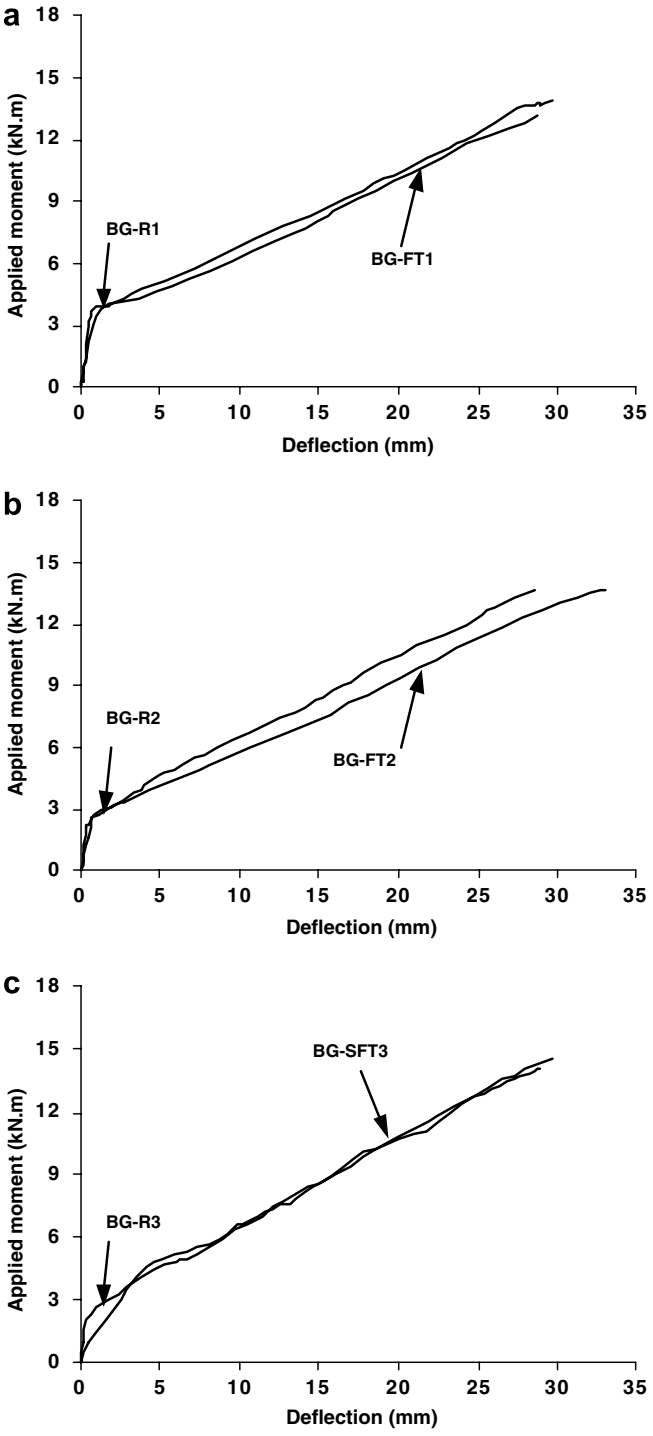

Fig. 10. Beams subjected to freeze–thaw cycles (Series III): (a) 100 freeze/thaw cycles (50 days), (b) 200 freeze/thaw cycles (100 days), (c) 360 freeze/thaw cycles (180 days).

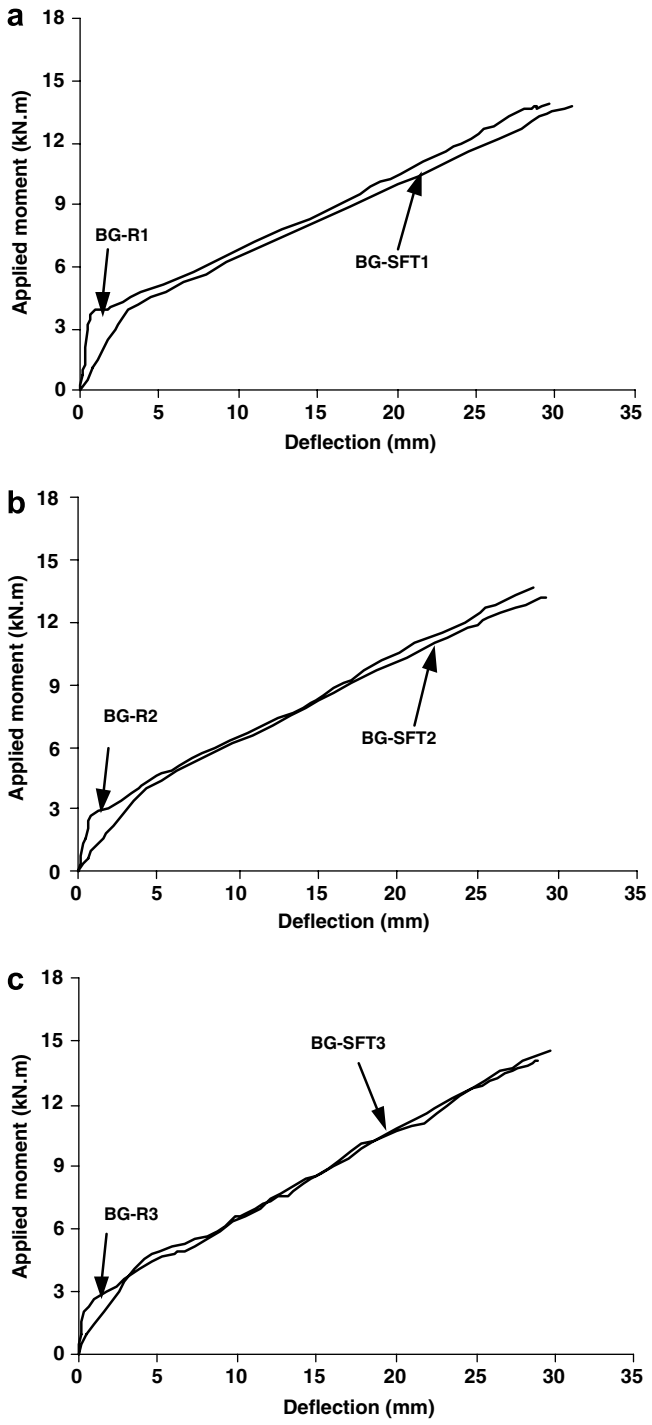

Fig. 11. Beams conditioned simultaneously under sustained load and freeze/thaw cycles (Series VI): (a) 100 freeze/thaw cycles (50 days), (b) 200 freeze/thaw cycles (100 days), (c) 360 freeze/thaw cycles (180 days).

respectively. Also, for these beams under the same conditions at service load limit, the mid-span deflection increased by 1.1%, 1.8%, and decrease by 2.2%, respectively.

All tested beams failed in tension by rupture of GFRP bars. This was expected since the concrete beams were under-reinforced. Fig. 12 shows the typical mode of failure. Strains in GFRP bars at service as well as at failure are also

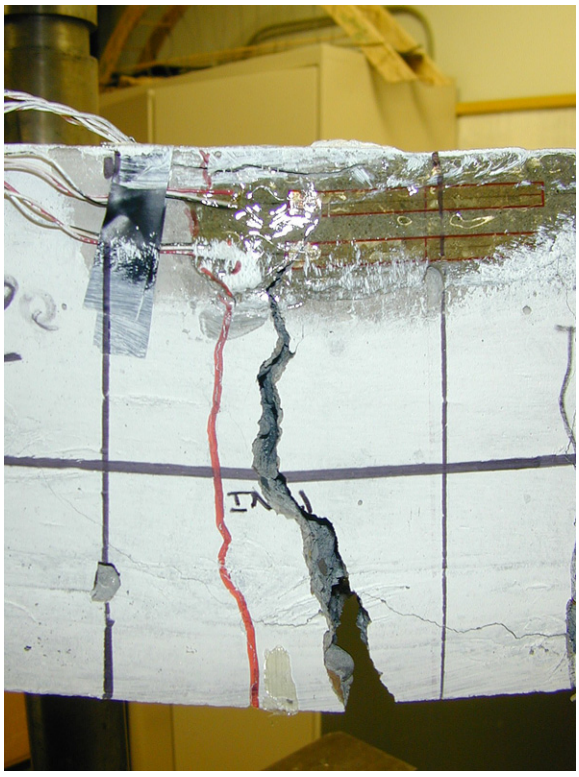

Fig. 12. Mode of failure (failed in tension by rupture of GFRP bars).

listed in Table 5. At failure, the strains in GFRP bars reached the proximity of the ultimate strain (1.8%).

5. Conclusions

A total of 21 concrete beams reinforced with GFRP bars were conditioned under the individual or coupled effect of sustained loads and freeze/thaw cycles (100, 200 and 360), and then tested to failure. Based on long-term test results, the following conclusions can be drawn:

1. The change in the ultimate capacity for the tested concrete beams after conditioning compared to unconditioned control ones was very small (±6%) and can be considered insignificant. However, the small increase in the capacity of concrete beams subjected to the individual effect of freeze/thaw cycles may be due to the increase in concrete strength as a result of longer and better curing.
2. Creep strain in the GFRP bars are less than 2.0 % of the initial value after 26 weeks (4360 h) of sustain tensile loading. This value was obtained under considerably high sustained stress of 27% of the ultimate tensile strength of the GFRP bars, which is about 2.33 times the currently recommended value by ACI 440.1R-06 for creep control.
3. The ACI 440.1R-06 equation to predict the long-term deflections due to creep and shrinkage over-estimates the experimental measured values.

Acknowledgements

The authors acknowledge the financial support received from the Natural Science and Engineering Research Council of Canada (NSERC), the Network of Centres of Excellence on Intelligent Sensing for Innovative Structures ISIS-Canada, and Centre de recherche sur les infrastructures en béton (CRIB). The authors wish to thank Pulturall Inc. (Thetford Mines, Quebec) for generously providing the FRP materials. Special thanks to the technicians at the Department of Civil Engineering, Université de Sherbrooke, for their help during the different stages of specimens' fabrication and testing.

References

[1] ACI 318-05/318R-05. Building code requirements for structural concrete and commentary. Farmington Hills, Michigan: American Concrete Institute; 2005. p. 391.
[2] ACI 440.1R-06. Guide for the design and construction of concrete reinforced with FRP bars. Farmington Hills, Michigan: American Concrete Institute; 2006. p. 41.
[3] Benmokrane B, Rahman H, editors. Durability of fibre reinforced polymer (FRP) composites for construction. In: Proceedings of the first international conference (CDCC 98), Sherbrooke, Québec, Canada, August 5–7, 1998. p. 692.
[4] Benmokrane B, El-Salakawy E, editors. Durability of fibre reinforced polymer (FRP) composites for construction. In: Proceedings of the second international conference (CDCC 02), Montréal, Québec, Canada, May 29–31, 2002. p. 715.
[5] CAN/CSA S806-02. Design and construction of building components with fibre reinforced polymers. Rexdale, Ontario: Canadian Standards Association; 2002. p. 177.
[6] El-Maaddawy T, Soudki K. Viability of using CFRP laminates to repair RC beams corroded under sustained load. In: Proceeding of the international symposium on FRP reinforcement for concrete structures (FRPRCS-6), Singapore, vol. 2, 2003. p. 855–64.
[7] GangaRao H, Kumar S. Design and fatigue response of concrete bridge decks reinforced with FRP rebars. In: Proceedings of the 2nd international symposium: non-metallic FRP reinforcement for concrete structures, Ghent, Belgium, August, 1995. p. 663–71.
[8] GangaRao HV, Vijay PV. Design of concrete members reinforced with GFRP bars. In: Proceedings of the 3rd international symposium on the use of non-metallic FRP reinforcement for concrete structures, vol. 1, 1997. p. 143–50.
[9] Gaona FA. Characterization of design parameters for composite reinforced concrete systems. Ph.D. thesis, Texas A&M University, December, 2003. p. 251.
[10] Gomez J, Castro B. Freeze–thaw durability of composites materials. Virginia Transportation Research Council Report, Richmond, VA, 1996.
[11] Humar J, Razaqpur G, editors. Advanced Composite materials in bridges and structures. In: Proceeding of the third international conference, Ottawa, Ontario, Canada, 2000. p. 876.
[12] Japan Society of Civil Engineers (JSCE). Recommendation for design and construction of concrete structures using continuous fiber reinforced materials. Concrete Engineering Series 23. In: Machida A, editor. Research committee on continuous fiber reinforcing materials, Tokyo, Japan, 1997.
[13] ISIS-M03-01. Reinforcing concrete structures with fibre reinforced polymers. The Canadian Network of Centres of Excellence on Intelligent Sensing for Innovative Structures. ISIS Canada, University of Winnipeg, Manitoba, 2001. p. 81.
[14] Lesko J. Freeze–thaw durability of polymer matrix composites in infrastructures. In: Proceedings, Duracosys 99, Brussels, Belgium, July 1999.
[15] Porter ML, Mehus J, Young KA, Barnes BA, O'Neil EF. Ageing degradation of fiber composite reinforcements for structural concrete. In: Second international conference on composites in infrastructure, ICCI'96, Tucson, AZ, 1996. p. 641–7.
[16] Pultrall Inc. ISOROD composite reinforcing rod. Technical Sheets, Thetford Mines, Quebec, 2000.
[17] Saadatmanesh H, Tannous FE. Durability of FRP and tendons. In: The 3rd international symposium on non-metallic reinforcement for concrete structures, Sapporo, Japan, vol. 2, 1997. p. 147–54.
[18] Schaefer B. Thermal and environmental effects on fiber reinforced polymer reinforcing bars and reinforced concrete. Master of Science Thesis, Texas A&M University, 2002.
[19] Soudki K, Green M. Freeze–thaw response of CFRP wrapped concrete. ACI Concrete Int 1997;19(4):39–42.